Antiferromagnetism and hidden order in isoelectronic doping of URu_2Si_2

M. N. Wilson,[1] T. J. Williams,[2] Y.-P. Cai,[1] A. M. Hallas,[1] T. Medina,[1] T. J. Munsie,[1] S. C. Cheung,[3] B. A. Frandsen,[3] L. Liu,[3] Y. J. Uemura,[3] and G. M. Luke[1,4]

[1]*Department of Physics and Astronomy, McMaster University, Hamilton, Ontario, Canada L8S 4M1*

[2]*Quantum Condensed Matter Division, Neutron Sciences Directorate, Oak Ridge National Laboratory, Oak Ridge, Tennessee 37831, USA*

[3]*Department of Physics, Columbia University, New York, New York 10027, USA*

[4]*Canadian Institute for Advanced Research, Toronto, Ontario, Canada M5G 1Z7*

(Received 28 November 2015; published 1 February 2016)

We present muon spin rotation (μSR) and susceptibility measurements on single crystals of isoelectronically doped $URu_{2-x}T_xSi_2$ (T = Fe, Os) for doping levels up to 50%. Zero field (ZF) μSR measurements show long-lived oscillations demonstrating that an antiferromagnetic state exists down to low doping levels for both Os and Fe dopants. The measurements further show an increase in the internal field with doping for both Fe and Os. Comparison of the local moment-hybridization crossover temperature from susceptibility measurements and our magnetic transition temperature shows that changes in hybridization, rather than solely chemical pressure, are important in driving the evolution of magnetic order with doping.

DOI: 10.1103/PhysRevB.93.064402

I. INTRODUCTION

Heavy fermion systems frequently exhibit interesting electronic ground states arising from complex hybridization between conduction electrons and localized f electrons [1]. Compounds containing uranium are particularly interesting as the Coulomb interaction, spin-orbit coupling, and $5f$ electron bandwidth are all of comparable energies, making exotic ground states possible [2]. A notable example of such a ground state is the hidden order (HO) arising in URu_2Si_2 below $T_0 = 17.5$ K that was first studied in 1985 [3,4]. The order in this state is termed "hidden" as, despite more than two decades of study, the order parameter for the 17.5 K transition has not yet been conclusively identified [2].

Early neutron scattering studies indicated that this state was antiferromagnetic with a moment of 0.02–0.04 μ_B per uranium [5,6]. However, other studies found unusual properties that could not be explained by simple antiferromagnetism, such as a gap opening up over a large portion of the Fermi surface indicated by specific heat [7] and infrared spectroscopy [8] measurements. Furthermore, the measured antiferromagnetic moment is too small to explain the $0.2R\ln 2$ per f.u. entropy change across the transition determined from specific heat measurements [7].

Subsequent neutron scattering measurements conducted under applied hydrostatic pressure demonstrated a first-order transition into a large moment antiferromagnetic state (LMAF) with a moment of 0.4 μ_B [9] that occurs at a critical pressure of 0.5–0.8 GPa [10]. μSR measurements under applied pressure have also confirmed this first-order transition to the LMAF state, and demonstrate no pressure dependence of the internal fields from 0.5 to 1.5 GPa [11]. In addition, μSR [12,13] and NMR measurements [14] show that the weak antiferromagnetic moment seen at ambient pressure can be explained by a small phase separated volume fraction of the pressure-induced antiferromagnetic state coexisting with the hidden order state. It is now widely accepted that this low moment antiferromagnetism is extrinsic to the hidden order state and is caused by inhomogeneous strain in measured crystals [15].

The origin of the entropy change in URu_2Si_2 seen from heat capacity measurements has recently been explained by a gap opening in the spin excitation spectrum at the transition, and does not require the presence of weak antiferromagnetism [16]. This gap is equivalent to the Fermi surface becoming gapped, and angle-resolved photoemission spectroscopy (ARPES) measurements [17,18] indicate that this gap arises from hybridization of the conduction band with the uranium $5f$ electrons. Scanning tunneling microscopy (STM) measurements [19] have lent support to this idea by observing a band splitting below the hidden order transition. However, these results have been disputed, with other STM researchers [17] claiming that the hybridization gap opens well above T_{HO} and hence cannot explain the hidden order state. This leaves the importance of the hybridization gap as one of the many unanswered questions of URu_2Si_2.

Despite these significant advances in the understanding of HO a viable theory has not yet been accepted to explain this state, although numerous theories have been advanced over the years (see Ref. [20] for a recent overview). In order to constrain such theories it is advantageous to further study the hidden order state through various experimental perturbations. One such perturbation that has been extensively applied to URu_2Si_2 is chemical doping. Previous studies have found that doping of the silicon site has only a weak effect on the electronic state which may be explained by a chemical pressure effect [21,22], while doping of the uranium [23,24] and ruthenium [25–28] sites cause much more dramatic changes in the behavior. This indicates that the electronic ground state depends much more strongly on d-f electron hybridization than it does on sp-f hybridization [22]. However, U-site doping is complicated as there is competition between dilution of the magnetic U atom, changes in lattice parameters, and hybridization all occurring with doping. This makes Ru-site doping interesting to study as it is a potentially simpler avenue to explore the effect of changing hybridization on the magnetic states.

Rhodium and rhenium doping are two cases that have been well studied, both of which suppress the HO state before 5% doping. However, the ground states that emerge after the suppression are distinctly different. For Re doping the

HO transition is suppressed by a 5% doping level, and above 7.5% doping a non-Fermi liquid ferromagnetic state emerges that persists up to high doping levels [29]. By contrast, Rh suppresses HO by 2% doping at which point a LMAF state emerges, which is in turn suppressed by 4% doping [30]. Above this doping level no magnetically ordered state is observed [30].

The Rh doped system has been a particularly valuable avenue to study the competition between the LMAF and HO states in the URu_2Si_2 system, as the doping allows the transition to be studied without the experimentally challenging aspects of applied external pressure. This has allowed productive studies of the high field behavior of the HO state (see Ref. [2] and references therein), as well as proposed identification of universal parameters that cause the transition between the HO and LMAF states [30].

Despite the potential insights gained by studying Re and Rh doping, the interpretation of results from both of these systems is made more difficult because these dopings change multiple potentially important parameters simultaneously. In particular, doping of Re or Rh will change the number of electrons in the system, the d-f hybridization, and the lattice constants of the system. In order to more easily understand the mechanisms behind the transitions between HO and other phases it is beneficial to have systems that change as few parameters as possible in order to isolate their effects. This makes the isoelectronic dopings, osmium and iron, interesting to study as one does not have to consider the effect of changing electron numbers in this system.

Fe doping of URu_2Si_2 has been studied for polycrystalline samples by Kanchanavatee *et al.* [31]. This work demonstrated that the full range of compositions $URu_{2-x}Fe_xSi_2$ from $x = 0$ to 2 can be produced, and that doping results in a monotonic decrease of the lattice parameters with no evidence for a change of structure. Furthermore, the temperature-doping phase diagram measured by bulk probes (specific heat, magnetization, and resistivity) shows an increase in transition temperature as a function of doping up to a maximum of 40 K. This increase parallels that of the pure compound under pressure, which led the authors to hypothesize a transition from HO to LMAF at a doping level of $x = 0.1$ and conclude that the effect of Fe doping on the system is fully explained by a chemical pressure effect [31]. However, the LMAF and HO states are largely indistinguishable to the bulk probes used in this study and the authors did not perform measurements with any microscopic probes that would allow the magnetic state to be identified, hence no firm conclusions could be drawn.

Recently, a second study has been published on Fe doping using neutron diffraction on single crystals [32]. In this work, elastic neutron scattering allowed the authors to identify a crossover from HO to AF at a doping level of $x = 0.1$ as would be expected from a chemical pressure argument. However, the moment of 0.8 μ_B per U that they observe is twice that seen in the pure material under pressure which indicates that chemical pressure is not the only factor governing the evolution of magnetism in this material. This discrepancy makes further study of Fe doping valuable to properly understand the HO to LMAF transition if it is to be used as an analog of the pressure induced transition.

A cursory study of polycrystalline $URu_{2-x}Os_xSi_2$ was first performed by Dalichaouch *et al.* in 1990 [27], and has been recently followed by a more detailed examination by Kanchanavatee *et al.* in 2014 [33]. These studies show that doping is possible up to $x = 1.2$ with no change in the structure and only a small increase in the lattice constant compared to the large decrease seen for Fe doping. Accompanying this small expansion of the lattice, the transition temperature dramatically increases up to a maximum of 50 K by $x = 1.2$. From resistivity and specific heat measurements Kanchanavatee *et al.* hypothesize a transition out of the HO state at $x = 0.2$. However, this study again did not involve any microscopic probes of magnetism and hence the true evolution of the magnetic ground state of $URu_{2-x}Os_xSi_2$ is still an open question.

In this paper we present the results of μSR and susceptibility measurements on $URu_{2-x}T_xSi_2$ (T = Fe, Os) single crystals for doping levels up to $x = 1$. Our measurements demonstrate that an antiferromagnetic state arises for both of these compounds at low doping levels and highlight the importance of hybridization to fully understand the evolution of magnetic order in this system.

II. EXPERIMENTAL METHODS

Samples measured in this study were single crystals grown by the Czochralski method at McMaster University from starting materials of depleted U, Ru(99.95%), Fe(99.99%), Os(99.8%), and Si(99.9999%). These growths were performed in a tri-arc furnace from a water-cooled copper hearth under argon gettered at 900 °C. After the growths, crystallinity was confirmed and sample alignment performed by Laue x-ray scattering measurements. Doping levels stated in this paper are the nominal doping levels taken from the masses of the materials originally reacted.

Magnetic susceptibility measurements were performed on cleaved plates of the crystals in a Quantum Design MPMS XL-3. These measurements provide a measure of the transition temperature from the paramagnetic state to hidden order or antiferromagnetism, however they cannot readily distinguish hidden order from antiferromagnetism.

μSR is a sensitive microscopic magnetic probe that can distinguish antiferromagnetism from hidden order, but cannot readily distinguish hidden order from paramagnetism. In this technique, spin polarized positive muons are injected one at a time into a sample where they penetrate a few hundred microns, rapidly thermalize, and stop at a Coulomb potential minimum in the material. Once stopped, each muon spin precesses in the local magnetic field until it decays with average lifetime of 2.2 μs and emits a positron preferentially in the direction of the muon spin at the time of decay. Detectors on either side of the sample register the decay of the positron and record the time interval between muon injection and decay. From many such events, a histogram of positron counts in both detectors, N_R and N_L, as a function of muon decay time is generated. Using these two histograms the asymmetry A is defined as $A = \frac{N_R - N_L}{N_R + N_L}$. This quantity gives a measure of how the muon polarization changes over time, and is limited by the physics of muon decay and instrumental factors to a maximum of about 0.3. The true maximum in any given experiment is

determined from the total oscillating asymmetry seen after applying a small field transverse to the muon polarization in the paramagnetic regime.

In zero applied magnetic field, paramagnetic samples, where there is no static magnetism and the spin dynamics are very fast, will show a nearly time-independent asymmetry, with deviations from this caused by nuclear moments. The HO state will also have this signature, as there is no ordering of magnetic moments to produce a local magnetic field. By contrast, long-range ordered magnetic states such as antiferromagnetism will show an oscillating asymmetry where the frequency gives the strength of the internal field at the muon stopping site, provided this field is not parallel to the initial muon polarization. The ratio of the maximum amplitude of the oscillating asymmetry to the instrumental maximum gives the fraction of the sample that is in the magnetic state (the magnetic volume fraction). The amplitude of this oscillating signal damps down over time as a result of inhomogeneities and dynamics of the internal field.

Our μSR measurements were performed on the M15 and M20 beam lines at TRIUMF laboratory in Vancouver. The LAMPF time-differential spectrometer was used, which provides a He-4 cryostat for temperatures between 2 and 300 K and a time resolution of 0.2 ns in an ultralow background apparatus. This apparatus vetoes muons that miss the sample, ensuring that almost all of the measured positrons come from muons that stop in the sample. For these measurements the single crystals were cleaved into slices roughly 0.5-mm thick along the c axis which were then mounted in a mosaic covering 1–2 cm^2 on thin mylar tape. The c axes were co-aligned facing the muon beam but no attempt was made to co-align the samples in the a-b plane. We fit our μSR data using the μSRfit software package [34].

III. RESULTS

Figures 1 and 2 show the results of the magnetization measurements in a field of 0.1 T ($H \parallel c$) on the Fe and Os doped samples, respectively. No significant differences were observed in any of these samples between field cooled and zero field cooled and hence only one set of measurements are shown. In these measurements a kink in the susceptibility indicates the transition into either the HO or LMAF states. The lower panels of these figures show plots of dM/dT to allow a more accurate determination of the temperature of this kink.

The measurements on the Fe doped samples show little change in the character of the transition with doping; the transition remains a relatively sharp peak in dM/dT up to higher dopings. The sharp peak is consistent with measurements on polycrystalline samples presented by Kanchanavatee *et al.* [31]. However, our measurements on single-crystal samples do not show evidence of the significant second peak seen in some of the polycrystalline samples in Ref. [31]. This likely indicates that those features were spurious results arising from disorder in the polycrystalline samples, as was also proposed by Das *et al.* [32]. Additionally, our $x = 0.3$ sample shows a significant low temperature upturn in the magnetization as well as the highest overall magnetization. During the crystal growth of this sample, a small number of needlelike protrusions were noticed on the outside of the crystal, likely indicating some

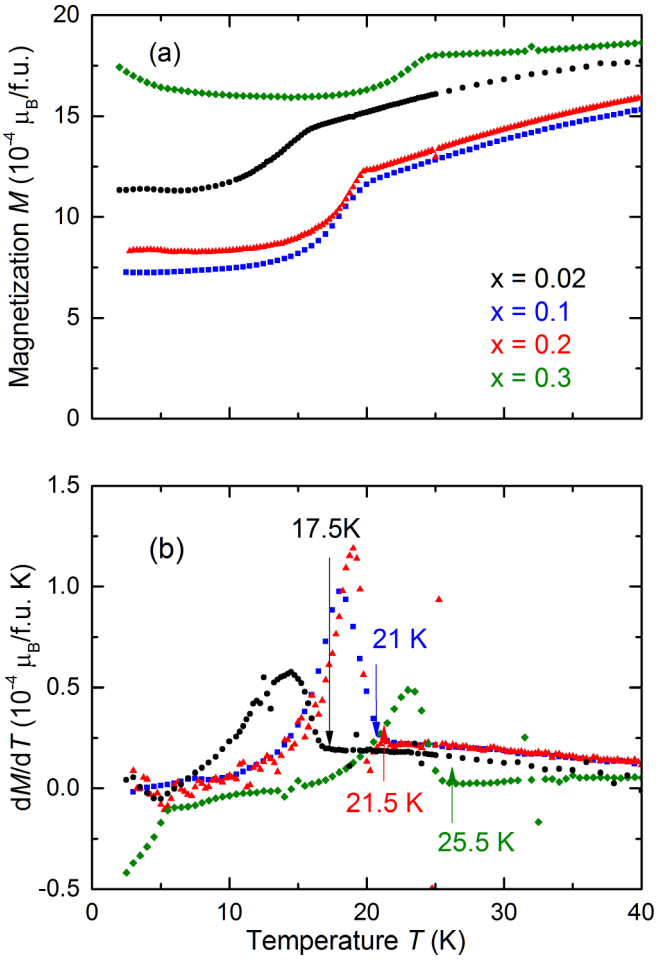

FIG. 1. (a) $URu_{2-x}Fe_xSi_2$ magnetization data measured in a field of $H = 0.1T \parallel c$ for $x = 0.02$ (black circles), 0.1 (blue squares), 0.2 (red triangles), and 0.3 (green diamonds). (b) Temperature derivative of the data shown in (a) arrows on plot (b) show the measured transition temperatures.

phase separation that would cause a paramagnetic background in the magnetization measurements, as observed. We attribute this to a lower than nominal silicon level in the melt arising from evaporation as silicon has the highest vapor pressure of the elements present [35] and the growth for this doping was held at high temperature for a significantly longer period than the others.

The measurements on our Os doped samples show a somewhat different evolution in the character of the transition with doping. Rather then staying as a sharp peak, the transition broadens significantly and shifts to higher temperature as the doping level increases. This is consistent with the broadened transition seen in polycrystalline samples at $x = 0.3$ and 0.4 [33].

μSR data for the Fe samples at 2 K measured with the muon spins initially perpendicular to the c axis of the crystals in zero applied field (ZF) is shown in Fig. 3. Measurements in Fig. 3(b) were taken with higher statistics to better resolve the faster relaxing signal. This data exhibits clear oscillations for all samples, indicating that there is static magnetism with the field along the c axis at the muon stopping site. The amplitude

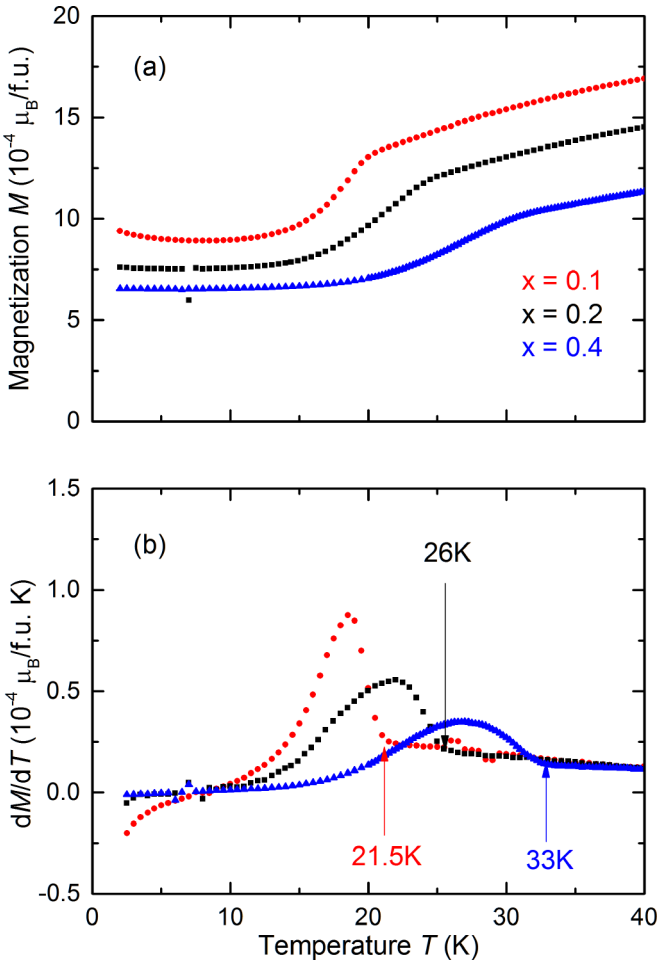

FIG. 2. (a) $URu_{2-x}Os_xSi_2$ magnetization data measured in a field of $H = 0.1T \parallel c$ for $x = 0.1$ (red circles), 0.2 (black squares), and 0.4 (blue triangles). (b) Temperature derivative of the data shown in (a). Arrows on plot (b) show the measured transition temperatures.

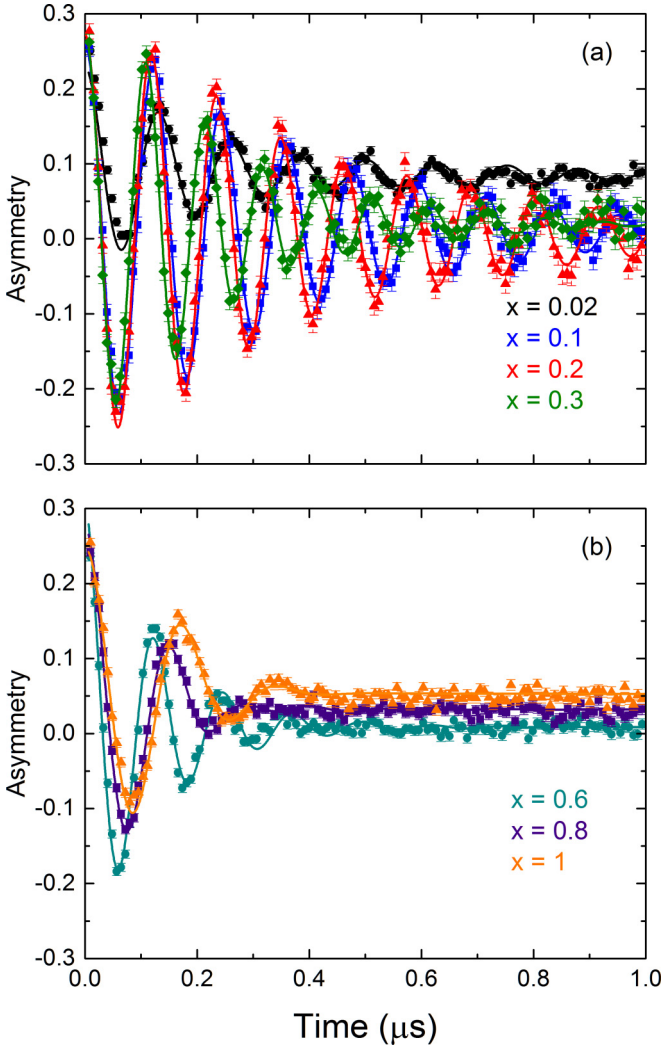

FIG. 3. $URu_{2-x}Fe_xSi_2$ μSR Data measured at $T = 2$ K in zero applied external field with the muon spins initially perpendicular to the c-axis for (a) $x = 0.02$ (black circles), 0.1 (blue squares), 0.2 (red triangles), and 0.3 (green diamonds) and (b) $x = 0.6$ (cyan circles), $x = 0.8$ (purple squares), and $x = 1$ (orange triangles). Solid lines in (a) show fits to Eq. (1) and those in (b) show fits to Eq. (2).

of the oscillations for the $x = 0.02$ sample is significantly lower than for the others and the asymmetry is shifted upwards by a nonrelaxing component. This indicates that the magnetic volume fraction is lower in this sample.

We found that applying a small field parallel to the c axis to any of these samples splits the observed internal field into two components separated by twice the applied field. This indicates that the magnetic order in these samples is antiferromagnetic. We also performed some measurements with the muon spins parallel to the c axis that show no oscillations for the low doping samples, indicating that the internal field is only along the c axis within the accuracy of our alignment. This is consistent with the antiferromagnetic phase seen in URu_2Si_2 under hydrostatic pressure [9] and by Das *et al.* in neutron scattering measurements on $URu_{2-x}Fe_xSi_2$ [32] which has magnetic moments along the c axis. However, it should be noted that while the direction of the internal field often matches the moment direction, this is not always the case and full comparison depends on knowledge of the muon stopping site which we do not have.

Despite the apparent similarity of this antiferromagnetic state to that of URu_2Si_2 under hydrostatic pressure, we found that the fitting of the ZF data at low doping was significantly improved with a two component fit compared to the single component fit used by Amato *et al.* for the pure compound [11]. We therefore fit the data for $x = 0.02$–0.3 shown in Fig. 3(a) using the equation

$$A = A_T\{0.5F\big[\cos(\gamma_\mu Bt)e^{-0.5(\sigma_1 t)^2} + \cos(\gamma_\mu BRt) \times e^{-0.5(\sigma_2 t)^2}\big] + (1 - F)\}. \quad (1)$$

In this model the ratio of the asymmetries of the two components was fixed to 0.5 for consistency between different samples as fits with free asymmetry were found to refine to values near 0.5. Addition of a second frequency for the higher dopings $x = 0.6$ to 1.0 did not improve the fits compared to the single component model given by the equation

$$A = A_T[F\cos(\gamma_\mu Bt)e^{-0.5(\sigma t)^2} + (1 - F)]. \quad (2)$$

TABLE I. Relaxation rates used to fit the 2 K μSR data in Fig. 3 for $URu_{2-x}Fe_xSi_2$ and the temperature independent ratio of the two internal fields used in fits to Eq. (1).

Doping x	R	σ_1 (μs^{-1}) at 2 K	σ_2 (μs^{-1}) at 2 K
0.02	0.86 ± 0.01	2.39 ± 0.08	5.37 ± 0.29
0.1	0.942 ± 0.008	1.95 ± 0.04	4.98 ± 0.13
0.2	0.93 ± 0.02	1.763 ± 0.04	4.39 ± 0.15
0.3	0.891 ± 0.004	2.822 ± 0.07	4.51 ± 0.12
0.6	–	7.57 ± 0.1	–
0.8	–	9.33 ± 0.18	–
1	–	7.04 ± 0.1	–

Therefore, Eq. (2) was used to fit the data in Fig. 3(b). In these equations A_T is the total asymmetry, B is the larger internal field, $\gamma_\mu = 135.53 \times 2\pi$ MHz/T is the muon gyromagnetic ratio, R is the ratio between the internal fields at the two muon sites, F is the magnetic volume fraction, and the σ_i are the relaxation rates. For each of the fits A_T and R were temperature independent parameters for each sample and the other parameters were allowed to vary with temperature.

The field ratio R varies between samples with no obvious doping dependence as shown in Table I. However, the relaxation rate also varies erratically from sample to sample, likely from differing amounts of disorder, and this will affect the fitting of a second frequency. Table I also shows the substantially larger single relaxation for the higher doped samples which obscures any possibility of fitting a second field to these data. We expect that a second frequency may still be present but increased disorder from growing crystals at high doping levels makes it impossible to distinguish.

Figure 4 shows plots of the fit average internal field [$0.5(B + RB)$ for the lower dopings] and magnetic fraction F. In all samples the internal field smoothly decreases from a maximum at low temperature to zero at the transition, showing second order behavior. The magnetic fraction for all samples except for the $x = 0.02$ is mostly temperature independent up until the transition where a sharp fall off occurs. This fraction is close to 1 for the $x = 0.1$–0.3 samples and slightly lower for the higher dopings. In contrast to the others, the $x = 0.02$ sample shows a substantially reduced F of 0.63 at 2 K. Furthermore, this sample shows different temperature dependence with a smooth continuous drop off in the magnetic fraction over the entire temperature range. This may indicate a continuous volume-wise transition out of the AF state as a function of temperature.

μSR data collected at $T = 5$ K in zero field with the muon spins initially perpendicular to the c axis for the Os doped samples are shown in Fig. 5(a). For these samples the data again show clear oscillations indicating similar static order. However, there is no evidence for a second internal field component in these samples. Therefore, we fit the data using Eq. (2) and show the internal field and magnetic volume fraction in Figs. 5(c) and 5(d). These plots show similar temperature dependence to the Fe doped samples again indicating a second order transition in all samples.

The comparison of two internal fields for Fe at low doping compared to one frequency in Os is illustrated by the Fourier transform in Fig. 5(b). This plot shows that while two frequencies appear in the Fe sample, the overall linewidth is similar for the Os sample. This means that the appearance of a second field for Os samples could be masked by the larger linewidth. Similarly, Table I shows that the relaxation rate (linewidth)

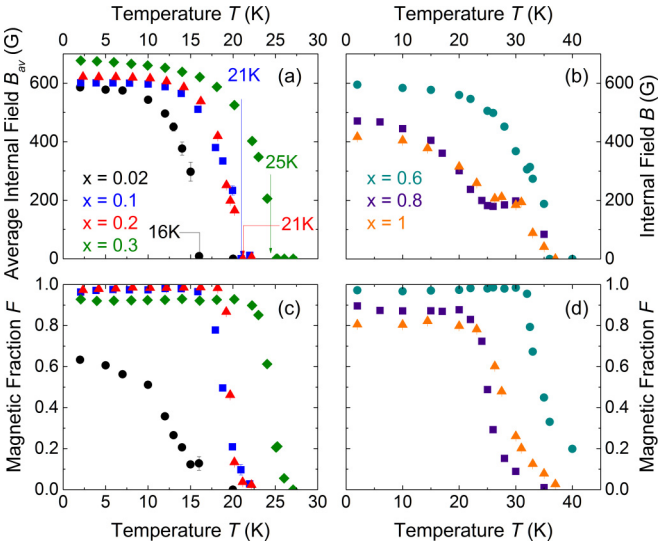

FIG. 4. Fitting parameters for the μSR data of $URu_{2-x}Fe_xSi_2$ measured in zero applied field with the muon spins perpendicular to the c-axis. (a) Average internal field $B_{av} = 0.5(B + RB)$ for dopings $x = 0.02$ (black circles), 0.1 (blue squares) 0.2 (red triangles) and 0.3 (green diamonds). (b) Internal field B for dopings $x = 0.6$ (cyan circles), 0.8 (purple squares) and 1 (orange triangles). (c) Magnetic volume fraction for dopings $x = 0.02$ (black circles), 0.1 (blue squares) 0.2 (red triangles) and 0.3 (green diamonds). (d) Magnetic volume fraction for dopings $x = 0.6$ (cyan circles), 0.8 (purple squares) and 1 (orange triangles).

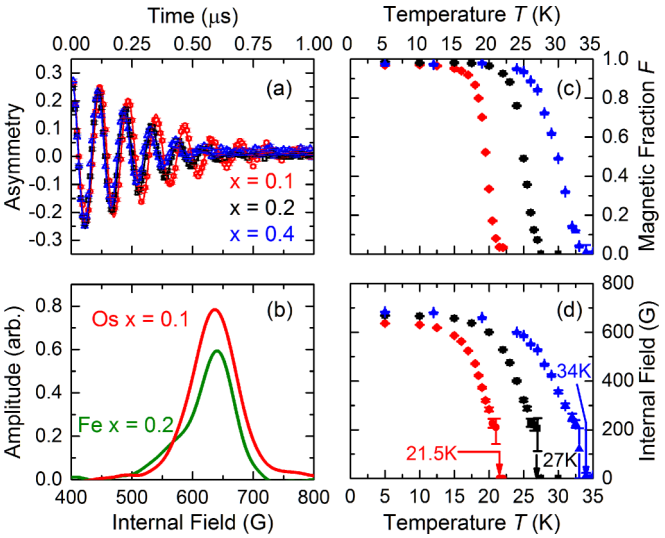

FIG. 5. $URu_{2x-}Os_xSi_2$ μSR data and fitting in zero external field measured with muon spins initially perpendicular to the c axis for $x = 0.1$ (red circles), 0.2 (black squares), and 0.3 (blue triangles). (a) μSR data measured at 5 K, (b) Fourier transform of $URu_{1.9}Os_{0.1}Si_2$ (red line) data measured at 5 K and $URu_{1.8}Fe_{0.1}Si_2$ (green line) data measured at 2 K, and (c) magnetic volume fraction F (d) internal field B. Solid lines in (d) correspond to fits to Eq. (2).

is much higher in the heavily doped Fe samples where two frequencies are not resolved. This is likely a result of chemical disorder in the samples and would explain why we cannot see two frequencies in these cases. A similar mechanism may explain the lack of a second field for the measurements under pressure done by Amato *et al.* [11]. In this case, the pressure was applied with an anvil cell using a transmitting medium that would be frozen at the relevant temperatures. This can cause nonuniformities in the applied pressure [36], which would introduce inhomogeneity in the samples, increasing the linewidth and masking the appearance of a second frequency. Furthermore, in any experiment with a pressure cell many muons are stopped outside the sample. This drops the signal to noise ratio of the data, further reducing the ability to resolve a possible second frequency. These explanations would allow for the magnetic state to be nearly identical in our Fe and Os samples as well as the pure URu_2Si_2 measured under pressure, despite the apparent differences in fitting.

The presence of a second internal field in any of these measurements indicates that the muons stop at two magnetically distinct sites at equivalent or near-equivalent Coulomb potential minima. The second magnetic site could either be explained by a more complex magnetic structure that breaks one of the symmetries of the underlying crystal lattice, or structural effects creating two muon sites. If this does appear only for doping, one possibility is that the Fe/Os atoms are being magnetically polarized and contributing to the moment seen by the muons. However, our measurements indicate that the relative volume fraction of the two magnetic sites is close to 50/50, which would not be expected if one of these was coming from the 1%–15% doping. Furthermore, UFe_2Si_2 and UOs_2Si_2 are both nonmagnetic so we would not expect Fe and Os polarization [37,38]. Future detailed measurements of the temperature and doping dependence of the lattice parameters and structure symmetry would help clarify this issue.

IV. DISCUSSION

The fit parameters in Figs. 4 and 5 show two important features. First, for most samples the low temperature magnetic volume fraction is close to one. This tells us that the magnetism we see must be attributed in each case to the bulk of the sample rather than to a small impurity effect. The small nonmagnetic volume that does appear could be attributed to muons stopping in parts of the sample holder rather than the sample itself or slight misalignment of the samples with respect to the incoming muon beam. In the heavily doped samples where the volume fraction appears somewhat reduced, a small signal also appears in measurements with the muon spin rotated parallel to the aligned c axis. Misalignment would explain both the signal in the $\mu||c$ measurements and the reduced signal/volume fraction for $\mu \perp c$ as the measured asymmetry varies as $\sin\theta$, where θ is the angle between the muon spins and the internal field.

Second, with the exception of the $x = 0.02$ Fe doped sample, the internal field falls off smoothly as a function of temperature to zero at a transition temperature consistent with that shown by the magnetization measurements. This indicates that the system transitions directly from the magnetically ordered to paramagnetic (PM) states without the transition

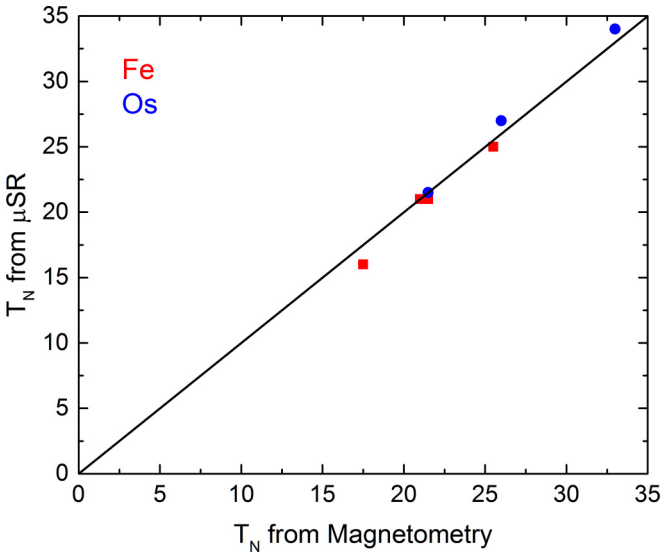

FIG. 6. Comparison of the transition temperatures measured by susceptibility to those measured by μSR for Fe doped samples (red squares) and Os doped samples (blue circles). The solid black line shows the expected 1:1 correspondence.

through HO that has been seen for intermediate pressures applied to URu_2Si_2 [11,29,39,40]. In the Fe $x = 0.02$ sample the transition temperature from μSR is 1.5 K lower than that measured by SQUID. This small discrepancy is unlikely to be caused by thermometry differences, as the same thermometry was used for μSR measurements of all other samples where the transition temperatures appear more consistent as shown by Fig. 6. Furthermore, the distinctly different temperature dependence in the magnetic volume fraction of this sample compared to the others leads us to believe that the magnetic state may not be the same. One explanation for these discrepancies is if this sample is in a mixed HO/AF state below 17.5 K, with the volume fraction of the AF state decreasing up until 16 K leaving a pure HO state in a 1.5 K range between 16 and 17.5 K. In the pressure-temperature phase diagram of pure URu_2Si_2 there exists a small temperature range where decreasing temperature first causes a transition into hidden order and then to antiferromagnetism, so it would not be unexpected to find a similar region at low Fe dopings in our system. However, as the transitions measured by both techniques are reasonably broad, and the temperature discrepancy is small, it is not possible to draw firm conclusions about the existence of both HO and AF at different temperatures in this sample. Further measurements on this doping with other techniques, particularly those that show a direct signature of the HO state such as inelastic neutron scattering, which has been used to distinguish the two under pressure [29], will be required to clarify this issue.

The overall behavior of the μSR data presented in this work is similar to that seen in measurements on URu_2Si_2 under hydrostatic pressure [11]. However, there are some notable differences. First, while the internal field measured at low temperature is comparable to that of Amato *et al.*, our measured internal fields for both Os and Fe increase with doping, while the internal field above some critical pressure is constant for URu_2Si_2 under pressure [11]. This difference in behavior

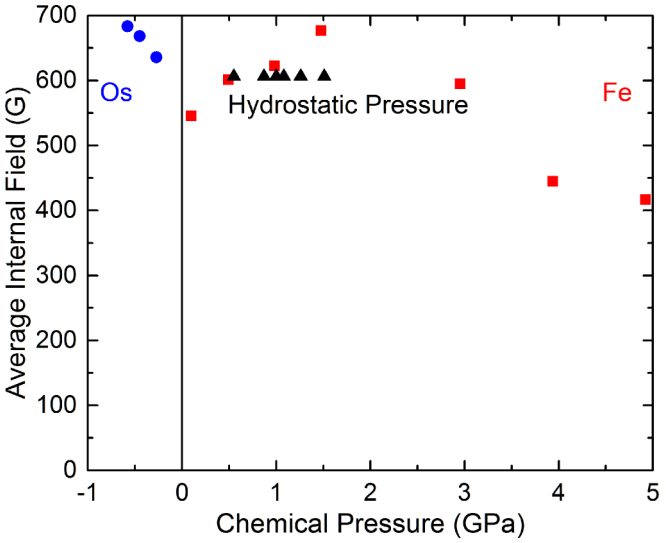

FIG. 7. Measured internal fields as a function of effective chemical pressure for Fe doped (red squares) and Os doped (blue circles), and as a function of applied hydrostatic pressure for pure URu_2Si_2 (black triangles) from Ref. [11]. Error bars are not shown as in all cases they would lie within the symbols.

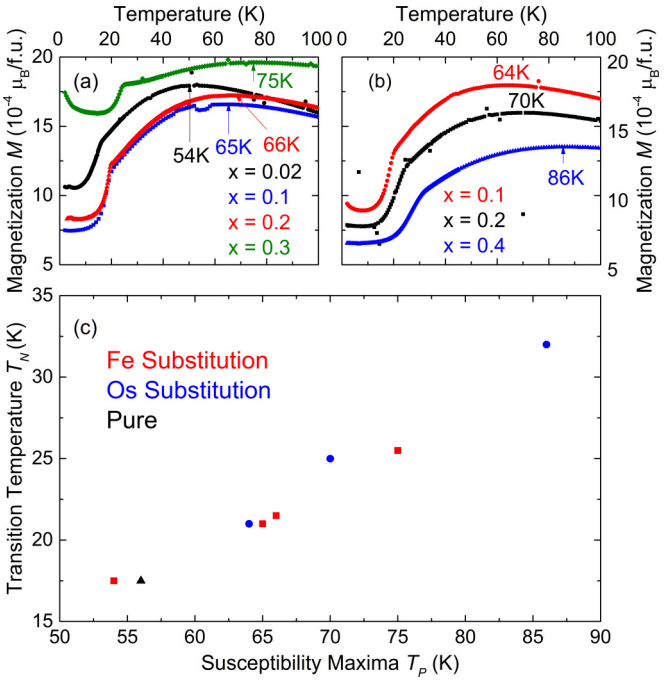

FIG. 8. High temperature susceptibility data showing the broad maxima that appears for (a) Fe doped samples, $x = 0.04$ (black circles), 0.1 (blue squares), 0.2 (red triangles), and 0.3 (green diamond) and (b) Os doped samples, $x = 0.1$ (red circles), 0.2 (black squares), and 0.4 (blue triangles). (c) A plot of T_N from susceptibility vs the temperature of this susceptibility maxima for Fe doped (red squares), Os doped (blue circles), and pure URu_2Si_2 (black triangle).

is clearly demonstrated in Fig. 7 showing the low temperature internal fields measured for all samples in this study plotted as a function of chemical pressure along with the data from Amato *et al.* For this plot the effective chemical pressure P_{ch} was calculated using $P_{ch} = (\Delta V)/(V_0)/\kappa$, where $\kappa = 5.2 \times 10^{-3}$ GPa^{-1} is the bulk modulus for pure URu_2Si_2 [41], ΔV is the unit cell volume change from pure URu_2Si_2 taken from the crystallographic data in Refs. [31,33] using our nominal doping levels, and V_0 is the unit cell volume of pure URu_2Si_2. This figure also indicates that the appearance of magnetic order cannot be attributed to chemical pressure across this system as the Os doped samples show similar internal fields at effective chemical pressures that are negative and whose magnitude is significantly lower than that for Fe doping. The Fe $x = 0.02$ sample also shows magnetic order despite being at an effective chemical pressure less than a quarter of the pressure required to generate the LMAF in pure URu_2Si_2. We would like to point out that as we have not done elemental analysis of the samples it is possible that the doping level of our $x = 0.02$ sample is slightly higher than the nominal value bringing it closer to the expected HO-AF border, but it is unlikely that the doping level is far enough off to fully resolve this discrepancy.

It has been proposed in the past that the transition between HO and LMAF is governed by the $\eta = c/a$ ratio as has been demonstrated for superconducting transitions in other f electron compounds [42], rather than uniform shrinking of the unit cell [33,43]. While both Fe and Os doping do increase η, the change is an order of magnitude smaller for Os doping than is seen for Fe doping or applied pressure. This indicates that the change in η alone cannot explain the development of magnetic order.

Susceptibility data on the lower doped samples show a clear broad maximum at high temperatures, shown in Figs. 8(a) and 8(b). Such a maximum is expected for heavy fermion compounds and arises from the crossover from local-moment magnetism at high temperature to the heavy fermion state at low temperatures caused by the hybridization of the conduction electrons with the core f electrons [1]. Hence, the temperature of this crossover T_{max} can be taken as a rough proxy for the strength of hybridization in these systems. Our data shows an increase in T_{max} with doping for both Os and Fe, which suggests that hybridization between the U f electrons and the valence electrons increases with doping for both cases. Furthermore, Fig. 8 shows a similar linear correlation between T_N and T_{max} in both cases. In contrast, measurements by two different groups of T_{max} as a function of pressure for pure URu_2Si_2 show conflicting results, with Nishioka *et al.* finding a pressure-independent value of approximately 60 K over a range where the magnetic transition temperature increases from 16 to 18.5 K [44], while Pfleiderer *et al.* find that T_{max} increases over this same pressure range [45]. It is therefore unclear whether or not our samples are behaving the same as URu_2Si_2 under pressure. However, the similarity in behavior between Os and Fe doping indicates that hybridization is the driving force in these transitions rather than chemical pressure.

Our results for Fe doping show some discrepancies with those reported recently by Das *et al.* using neutron scattering on crystals that should be similar to ours [32]. First, our internal fields increase with doping, while the results of Das *et al.* show either doping independence or a slight decrease with doping. Second, our measured internal field is roughly consistent with URu_2Si_2 under pressure, while Das *et al.* report a magnetic moment up to twice that measured for the LMAF in URu_2Si_2. Finally, we see similar magnetism down

to low doping levels while Das *et al.* see weakening of the magnetism below $x = 0.1$.

The first discrepancy could be explained by slight changes to the muon stopping site with doping. If the muons systematically stop closer to the magnetic U atoms as the Fe doping increases, this would cause a small increase in our observed internal field even if the magnetic moments are constant or slightly decreasing. However, in a simplistic viewpoint the dopant Fe atoms should have electron orbitals with smaller spatial extent than the Ru, and hence one would expect the muon stopping sites to move closer to the Fe atoms and further from the magnetic U ions. This would cause a decrease in the measured internal field rather than an increase. Detailed numerical calculations of the likely muon stopping sites would be required to quantitatively determine the effect of the Fe doping. Another explanation for the doping dependence is Fe site magnetism contributing to the internal field, which could potentially be clarified with Mössbauer measurements that could directly measure the Fe magnetism.

The second discrepancy is difficult to reconcile. While μSR cannot provide a numerical value of the magnetic moment without knowledge of the muon stopping site which we do not have, the comparison between the measured internal fields of samples with very similar structures should give a good idea of how the magnetic moment changes between these samples. Therefore, the Fe $x = 0.1$ sample should be reasonably comparable to the pure compound under pressure and hence seeing a similar internal field here should indicate that the magnetic moments are the same. While the doping could change the muon stopping site somewhat between pure URu_2Si_2 and the Fe $x = 0.1$ sample, the structure and lattice constants remain mostly the same and it seems unlikely that this would be a large enough effect to cut the measured internal field in half to make our results consistent with the magnetic moment measured by Das *et al.* One possibility is that there is signal intensity at the magnetic Bragg peak positions from multiple scattering that Das *et al.* may not have taken into account and would artificially inflate the calculated magnetic moments.

The final discrepancy of our data showing magnetism down to lower doping levels may come down to slight variations in doping levels or internal strain between different crystals. In particular, the doping levels we state are the nominal dopings and were not independently measured so there may be some small discrepancies. However, our results are not entirely inconsistent with those of Das *et al.* They report that there is some magnetic scattering still appearing in the lower doped samples, it is just substantially reduced. This could come from magnetic moments that are the same as those measured in higher doping samples, but with a reduced magnetic volume fraction, as the Bragg peak intensity cannot distinguish volume fraction from magnetic moment. A reduced volume fraction with similar magnetic moment would be qualitatively consistent with the results we show for our nominal Fe $x = 0.02$ sample.

V. CONCLUSION

In conclusion, we have presented μSR measurements which demonstrate that $URu_{2-x}T_xSi_2$ (T = Os, Fe) display antiferromagnetic order. This order persists down to low doping levels, with our Fe $x = 0.02$ sample showing a lowered magnetic volume fraction that may indicate coexistence of HO and AF in this sample. Furthermore, the magnetic order persists down to Fe doping levels below that expected by a chemical pressure argument, and for Os dopings representing negative chemical pressure, which shows that the hidden order is very fragile and can easily be destroyed by even isoelectronic doping. These measurements, combined with the local moment-hybridization crossover temperature from susceptibility, demonstrate that magnetic order in isoelectronic doping is driven by changes in hybridization rather than purely structural changes.

ACKNOWLEDGMENTS

We thank Dr. G. D. Morris, Dr. B. S. Hitti and Dr. D. J. Arseneau (TRIUMF) for their assistance with the μSR measurements. Work at McMaster university was supported by the Natural Sciences and Engineering Research Council of Canada and the Canadian Foundation for Innovation. M.N.W. acknowledges support from the Alexander Graham Bell Canada Graduate Scholarship program. T.J.W. acknowledges support from the Wigner Fellowship program at Oak Ridge National Laboratory. A.M.H. acknowledges support from the Vanier Canada Graduate Scholarship program. G.M.L. acknowledges support from the Canadian Institute for Advanced Research. The Columbia University group acknowledges support from NSF DMR-1436095 (DMREF) and OISE-0968226 (PIRE), JAEA Reimei project, and Friends of U Tokyo, Inc.

[1] G. R. Stewart, Rev. Mod. Phys. **56**, 755 (1984).
[2] J. A. Mydosh and P. M. Oppeneer, Rev. Mod. Phys. **83**, 1301 (2011).
[3] W. Schlabitz, J. Baumann, B. Pollit, U. Rauchschwalbe, H. M. Mayer, U. Ahlheim, and C. D. Bredl, Z. Phys. B: Condens. Matter **62**, 171 (1986).
[4] T. T. M. Palstra, A. A. Menovsky, J. van den Berg, A. J. Dirkmaat, P. H. Kes, G. J. Nieuwenhuys, and J. A. Mydosh, Phys. Rev. Lett. **55**, 2727 (1985).
[5] C. Broholm, J. K. Kjems, W. J. L. Buyers, P. Matthews, T. T. M. Palstra, A. A. Menovsky, and J. A. Mydosh, Phys. Rev. Lett. **58**, 1467 (1987).
[6] E. D. Isaacs, D. B. McWhan, R. N. Kleiman, D. J. Bishop, G. E. Ice, P. Zschack, B. D. Gaulin, T. E. Mason, J. D. Garrett, and W. J. L. Buyers, Phys. Rev. Lett. **65**, 3185 (1990).
[7] M. B. Maple, J. W. Chen, Y. Dalichaouch, T. Kohara, C. Rossel, M. S. Torikachvili, M. W. McElfresh, and J. D. Thompson, Phys. Rev. Lett. **56**, 185 (1986).
[8] D. A. Bonn, J. D. Garrett, and T. Timusk, Phys. Rev. Lett. **61**, 1305 (1988).
[9] H. Amitsuka, M. Sato, N. Metoki, M. Yokoyama, K. Kuwahara, T. Sakakibara, H. Morimoto, S. Kawarazaki, Y. Miyako, and J. A. Mydosh, Phys. Rev. Lett. **83**, 5114 (1999).

[10] N. P. Butch, J. R. Jeffries, S. Chi, J. B. Leão, J. W. Lynn, and M. B. Maple, Phys. Rev. B **82**, 060408 (2010).
[11] A. Amato, M. J. Graf, A. de Visser, H. Amitsuka, D. Andreica, and A. Schenck, J. Phys.: Condens. Matter **16**, S4403 (2004).
[12] D. E. MacLaughlin, D. W. Cooke, R. H. Heffner, R. L. Hutson, M. W. McElfresh, M. E. Schillaci, H. D. Rempp, J. L. Smith, J. O. Willis, E. Zirngiebl, C. Boekema, R. L. Lichti, and J. Oostens, Phys. Rev. B **37**, 3153 (1988).
[13] G. M. Luke, A. Keren, L. P. Le, Y. J. Uemura, W. D. Wu, D. Bonn, T. Taillefer, J. D. Garret, and Y. Onuki, Hyperfine Interact. **85**, 397 (1994).
[14] K. Matsuda, Y. Kohori, T. Kohara, K. Kuwahara, and H. Amitsuka, Phys. Rev. Lett. **87**, 087203 (2001).
[15] H. Amitsuka, K. Matsuda, I. Kawasaki, K. Tenya, M. Yokoyama, C. Sekine, N. Tateiwa, T. C. Kobayashi, S. Kawarazaki, and H. Yoshizawa, J. Magn. Magn. Mater. **310**, 214 (2007).
[16] C. R. Wiebe, J. A. Janik, G. J. MacDougall, G. M. Luke, J. D. Garrett, H. D. Zhou, Y.-J. Jo, L. Balicas, Y. Qiu, J. R. D. Copley, Z. Yamani, and W. J. L. Buyers, Nat. Phys. **3**, 96 (2007).
[17] A. F. Santander-Syro, M. Klein, F. L. Boariu, A. Nuber, P. LeJay, and F. Reinert, Nat. Phys. **5**, 637 (2009).
[18] S. Chatterjee, J. Trinckauf, T. Hänke, D. E. Shai, J. W. Harter, T. J. Williams, G. M. Luke, K. M. Shen, and J. Geck, Phys. Rev. Lett. **110**, 186401 (2013).
[19] A. R. Schmidt, M. H. Hamidian, P. Wahlm F. Meier, A. Balatsky, J. D. Garret, T. J. Williams, G. M. Luke, and J. C. Davis, Nature (London) **465**, 570 (2010).
[20] J. A. Mydosh and P. M. Oppeneer, Philos. Mag. **94**, 3640 (2014).
[21] S. K. Dhar, R. J. Begum, P. Raj, P. Suryanarayana, L. C. Gupta, and R. Vijayaraghavan, Solid State Commun. **83**, 965 (1992).
[22] J.-G. Park and B. R. Coles, J. Phys.: Condens. Matter **6**, 1425 (1994).
[23] M. Ocko and J.-G. Park, Physica B **230–232**, 71 (1997).
[24] H. Amitsuka, K. Kuwahara, M. Yokoyama, K. Tenya, T. Sakakibara, M. Mihalik, and A. A. Menovský, Phys. B: Condens. Matter **281–282**, 326 (2000).
[25] H. Amitsuka, K. Hyomi, T. Nishioka, Y. Miyako, and T. Suzuki, J. Magn. Magn. Mater. **76–77**, 168 (1988).
[26] Y. Dalichaouch, M. B. Maple, R. P. Guertin, M. V. Kuric, M. S. Torikachvili, and A. L. Giorgi, Physica B **163**, 113 (1990).
[27] Y. Dalichaouch, M. B. Maple, J. W. Chen, T. Kohara, C. Rossel, M. S. Torikachvili, and A. L. Giorgi, Phys. Rev. B **41**, 1829 (1990).
[28] J.-G. Park, J. Phys.: Condens. Matter **6**, 3403 (1994).
[29] N. P. Butch and M. B. Maple, J. Phys.: Condens. Matter **22**, 164204 (2010).
[30] M. Yokoyama, H. Amitsuka, S. Itoh, I. Kawasaki, K. Tenya, and H. Yoshizawa, J. Phys. Soc. Jpn. **73**, 545 (2004).
[31] N. Kanchanavatee, M. Janoschek, R. E. Baumbach, J. J. Hamlin, D. A. Zocco, K. Huang, and M. B. Maple, Phys. Rev. B **84**, 245122 (2011).
[32] P. Das, N. Kanchanavatee, J. S. Helton, K. Huang, R. E. Baumbach, E. D. Bauer, B. D. White, V. W. Burnett, M. B. Maple, J. W. Lynn, and M. Janoschek, Phys. Rev. B **91**, 085122 (2015).
[33] N. Kanchanavatee, B. D. White, V. W. Burnett, and M. B. Maple, Philos. Mag. **94**, 3681 (2014).
[34] A. Suter and B. M. Wojek, Phys. Proc. **30**, 69 (2012).
[35] R. E. Honig, RCA Rev. **23**, 567 (1962).
[36] W. Yu, A. A. Aczel, T. J. Williams, S. L. Bud'ko, N. Ni, P. C. Canfield, and G. M. Luke, Phys. Rev. B **79**, 020511(R) (2009).
[37] A. Szytula, M. Slaski, B. Dunlap, Z. Sungaila, and A. Umezawa, J. Magn. Magn. Mater. **75**, 71 (1988).
[38] T. T. M. Palstra, A. A. Menovsky, G. J. Nieuwenhuys, and J. A. Mydosh, J. Magn. Magn. Mater. **54–57**, 435 (1986).
[39] F. Bourdarot, S. Raymond, and L.-P. Regnault, Philos. Mag. **94**, 3702 (2014).
[40] E. Hassinger, G. Knebel, K. Izawa, P. Lejay, B. Salce, and J. Flouquet, Phys. Rev. B **77**, 115117 (2008).
[41] K. Kuwahara, H. Sagayama, K. Iwasa, M. Kohgi, S. Miyazaki, J. Nozaki, J. Nogami, M. Yokoyama, H. Amitsuka, H. Nakao, and Y. Murakami, Acta Phys. Pol. B **34**, 4307 (2003).
[42] C. Pfleiderer, Rev. Mod. Phys. **81**, 1551 (2009).
[43] M. Yokoyama, H. Amitsuka, K. Tenya, K. Watanabe, S. Kawarazaki, H. Yoshizawa, and J. A. Mydosh, Phys. Rev. B **72**, 214419 (2005).
[44] T. Nishioka, H. Mukai, S. Nakamura, G. Motoyama, Y. Ushida, and N. K. Sato, J. Phys. Soc. Jpn. **69**, 2415 (2000).
[45] C. Pfleiderer, J. A. Mydosh, and M. Vojta, Phys. Rev. B **74**, 104412 (2006).